The "Sweet" Side of the Protein Corona: Effects of Glycosylation on Nanoparticle–Cell Interactions

Sha Wan,[†] Philip M. Kelly,[†] Eugene Mahon,[†] Henning Stöckmann,[‡] Pauline M. Rudd,[‡] Frank Caruso,[§] Kenneth A. Dawson,[†] Yan Yan,[*,§] and Marco P. Monopoli[*,†]

[†]Centre for BioNano Interactions, School of Chemistry and Chemical Biology, University College Dublin, Dublin 4, Ireland, [‡]NIBRT, GlycoScience Group, NIBRT—The National Institute for Bioprocessing Research and Training, Fosters Avenue, Mount Merrion, Blackrock, Co. Dublin, Ireland, and [§]ARC Centre of Excellence in Convergent Bio-Nano Science and Technology, and the Department of Chemical and Biomolecular Engineering, The University of Melbourne, Parkville, Victoria 3010, Australia

ABSTRACT The significance of a protein corona on nanoparticles in modulating particle properties and their biological interactions has been widely acknowledged. The protein corona is derived from proteins in biological fluids, many of which are glycosylated. To date, the glycans on the proteins have been largely overlooked in studies of nanoparticle–cell interactions. In this study, we demonstrate that glycosylation of the protein corona plays an important role in maintaining the colloidal stability of nanoparticles and influences nanoparticle–cell interactions. The removal of glycans from the protein corona enhances cell membrane adhesion and cell uptake of nanoparticles in comparison with the fully glycosylated form, resulting in the generation of a pro-inflammatory milieu by macrophages. This study highlights that the post-translational modification of proteins can significantly impact nanoparticle–cell interactions by modulating the protein corona properties.

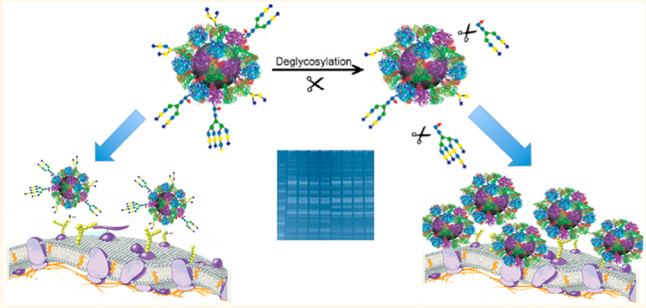

KEYWORDS: nanoparticle · glycosylation · protein corona · macrophage · adhesion · internalization

Advances in engineering functional structures at the nanoscale have led to the generation of a wide range of nanoparticles, including silica (SiO_2) nanoparticles, gold nanoparticles, and polymeric nanoparticles.[1] With their dimension in the size ranging from 1–100 nm, these nanoparticles have opened up exciting avenues in a broad range of biomedical applications, including targeted drug delivery.[2–5] For the continued development of nanoparticle-based biomedicine, an understanding of the complex interactions between nanoparticles and biological systems is essential.

It is now widely acknowledged that nanoparticles adsorb many biomolecules (mainly proteins) upon exposure to biological milieu, resulting in the formation of a new interface termed the "protein corona".[6–14] Increasing evidence has shown that the protein corona regulates nanoparticle–cell recognition, and hence plays important roles in modulating nanoparticle mobility and toxicity.[15–20] For example, the adsorption of proteins on nanoparticles has been shown to reduce nanoparticle cell membrane adhesion, mitigating the disruption of cell membranes by bare nanoparticles.[21] Alternatively, the adsorbed proteins have been shown to negatively impact on the specificity of nanoparticles to targeted cells, resulting in the loss or reduction of the targeting capability of surface functionalized nanoparticles.[22] In addition, nanoparticles can induce conformational changes in the adsorbed proteins, which in turn trigger *de novo* nanoparticle–cell recognition and initiate alternative cell signal transduction.[23–25] Collectively, the biological relevance of a protein corona is intimately linked with its molecular properties. These molecular details not only include the macroscopic composition of the adsorbed proteins, but also their structure, conformation and organization.

One of the most abundant post-translational modifications of proteins is glycosylation. It is estimated that over 50% of all

* Address correspondence to marco.monopoli@cbni.ucd.ie, yanyan@unimelb.edu.au.

Received for review October 23, 2014 and accepted January 19, 2015.

Published online January 19, 2015
10.1021/nn506060q

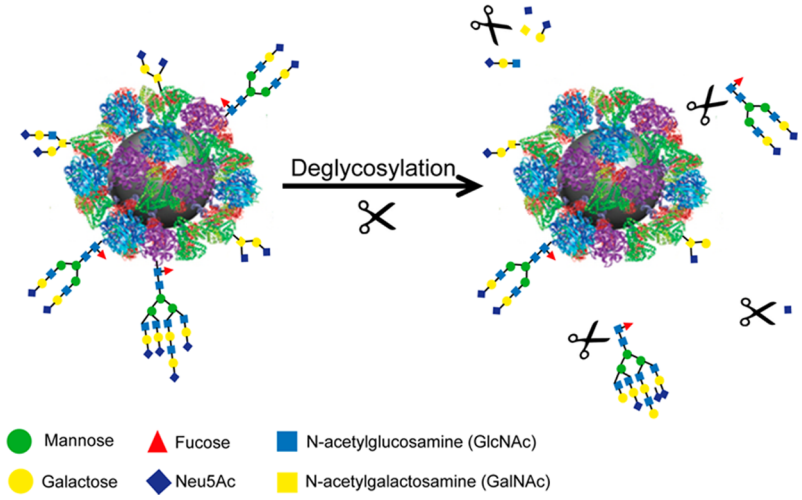

Scheme 1. *In situ* enzymatic deglycosylation of the hard protein corona on nanoparticles. Nanoparticle−protein complexes are treated with a mixture of endoglycosidases and exoglycosidases to remove the outermost surface glycans while the proteins are retained on the nanoparticles.

human proteins are glycosylated.[26] In eukaryotic cells most glycosylation events occur in the endoplasmic reticulum (ER) along the ER−Golgi−plasma membrane trafficking pathway catalyzed by a series of glycosidases and glycotransferases. In general the attached glycans play a critical role in maintaining protein stability and conformation, facilitating protein folding and trafficking, as well as regulating protein immunogenicity and protein−protein interactions.[27,28] Despite the ubiquitous presence of glycans in proteins, little is known about the organization of the glycans in the nanoparticle protein corona and their effects on nanoparticle−cell interactions.

Herein, we investigate the roles of glycans at the outermost surface of the hard corona in mediating nanoparticle−cell interactions using a model nanoparticle system (SiO_2 nanoparticles). A protein corona derived from human plasma has been chosen for the model corona, as most proteins in the blood plasma are heavily glycosylated, and intravenous administration of nanoparticles is one of the most relevant delivery routes for many biological applications. We incubated SiO_2 nanoparticles with complete human plasma and applied washes to obtain the hard corona-nanoparticles.[29] Subsequently, the nanoparticles coated with the hard corona are enzymatically deglycosylated *in situ* (Scheme 1). The deglycosylation results in an increase in the electrophoretic mobility of corona proteins observed by sodium dodecyl sulfate polyacrylamide gel electrophoresis (SDS-PAGE). Additionally, fluorescently labeled lectins have been used to monitor the loss of the glycans and to probe the remaining glycan structures on the corona. These studies have revealed that deglycosylation *in situ* partially removes glycans from the corona (even with extended incubation), leading to presentation of new internal glycan structures. Finally, cell membrane adhesion, uptake and cytokine stimulation of the deglycosylated nanoparticle−protein complexes has been evaluated using THP-1 differentiated macrophages. Our data show that in comparison to the full corona, the deglycosylation of corona proteins enhances nanoparticle−cell adhesion and stimulates pro-inflammatory responses by macrophages.

RESULTS AND DISCUSSION

Fluorescently labeled SiO_2 nanoparticles of 56 nm diameter, as measured by transmission electron microscopy (TEM) (Figure S1), were incubated with human plasma to form a protein corona. The particle size, polydispersity, and zeta-potential were determined by dynamic light scattering (DLS) and differential centrifugal sedimentation (DCS). The DLS data showed that the adsorption of proteins resulted in an increase of the nanoparticle size (Figure 1a and Table S1), and a change in correlogram and cumulation fit of DLS measurements (Figure S2), which has consistently been seen with other nanoparticles.[21,29] In good agreement, DCS measurements exhibited a change in sedimentation time due to the corona formation (Figure S3a). The zeta-potential of the nanoparticles decreased from −18 to −10 mV upon the formation of the protein corona (Figure 1b and Table S1). Such neutralization effects of the protein corona on particle surface charge have been observed in both negatively and positively charged nanoparticles,[29,30] as electrostatic interaction between nanoparticles and proteins is one of the main forces driving the formation of the protein corona,[6] where colloidal stability is nevertheless maintained through steric stabilization effects during the protein adsorption.

To obtain a set of nanoparticle−protein complexes with various degrees of glycosylation, the corona-nanoparticles were treated with a glycosidase mixture (comprising PNGase F, O-glycosidase, neuraminidase,

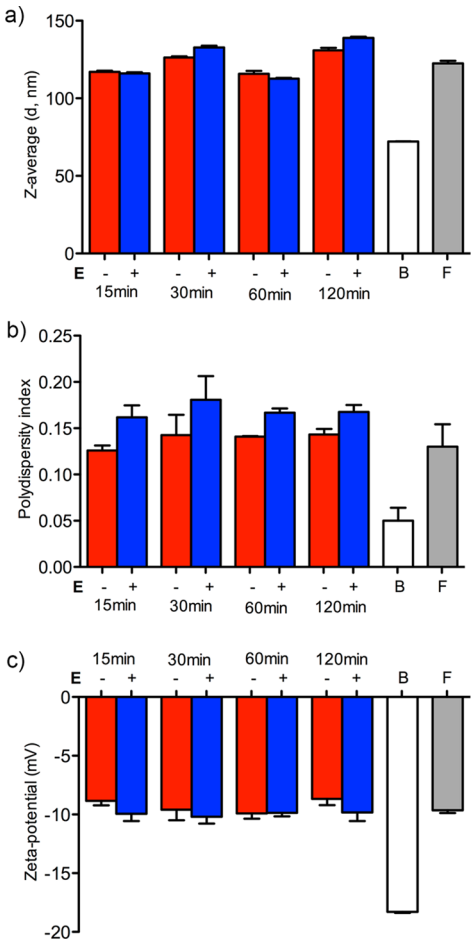

Figure 1. Characterization of SiO_2 nanoparticle−protein complexes before and after deglycosylation: z-average hydrodynamic diameter (a), polydispersity index (b), and zeta-potential (c). Nanoparticle-complexes were deglycosylated *in situ* for various time periods (15, 30, 60, and 120 min, respectively, E+). E− represents nonenzyme-treated controls. Bare nanoparticles and full protein corona-nanoparticles were referred to as B and F, respectively. Data of z-average and zeta-potential are the mean ± standard error of three measurements.

β1−4 galactosidase, and β-*N*-acetylglucosaminidase) for different time intervals, removing both N-linked and O-linked glycans at the outermost surface of the complexes. For comparison, equivalent corona-nanoparticles were exposed to the same deglycosylation reaction conditions in the absence of glycosidases. Using the cumulant fitting method for DLS, polydispersity index (PDI) was used to quantify relative distribution width. It was shown that the deglycosylation led to a slight increase in the polydispersity of the nanoparticle−protein complexes (Figure 1b and Table S1). The cumulation fits and correlograms of the DLS measurements were further analyzed using a method described (Figure S4, S5).[31] It was shown that exposure of the nanoparticles with deglycosylation enzymes resulted in a significant and progressive change in the nanoparticle diffusion due to the loss of glycans (Figure S4). In contrast, exposure of the NP protein corona complexes over time in the same buffer without the glycosidases did not result in any significant changes in diffusion proprieties, suggesting that these complexes are stable over time (Figure S5). Furthermore, DCS measurements demonstrated that a progressive shift in apparent diameter occurred when the nanoparticle−protein corona complexes were exposed for increasing amount of time to glycosidases (Figure S3b), whereas the control samples (in the absence of glycosidases) remained unchanged (Figure S3c). Combined, these results have suggested that the colloidal stability of the glycosylated and deglycosylated nanoparticle−protein complexes is well maintained throughout the experimental conditions. In addition, all of the nanoparticle−protein complexes exhibited a similar neutral zeta-potential of approximately −10 mV at pH 7.4 and the deglycosylation did not result in significant alterations in their zeta-potential (Figure 1c). Taken together, these data suggest that steric stabilization is one of the main driving forces for the colloidal stability of the nanoparticle−protein complexes. Glycans are singular in organizing the hydration of biomolecules and therefore keeping the nanoparticles disperse. The loss of glycans at the outermost surface of the protein corona can facilitate nonselective hydrophobic and electrostatic interaction between protein surfaces, leading to a decrease of the overall stability of the nanoparticle−protein complexes.

To confirm that the enzymatic deglycosylation of the protein corona had indeed occurred *in situ*, the proteins from the hard corona were subsequently eluted from the nanoparticles and separated by SDS-PAGE. It was expected that deglycosylated proteins would increase their electrophoretic mobility relative to their fully glycosylated forms. Direct comparison between the enzyme-treated and nonenzyme controls revealed several reproducible differences in the range between 62−14 kDa (indicated by arrows in Figure 2). In particular, the proteins near the 28 and 14 kDa bands appeared to undergo subtle progressive changes with an increase in the deglycosylation reaction time (Figure 2), suggesting that different degrees of glycosylation remained in the nanoparticle−protein complexes. Extending the incubation time or increasing the concentrations of the deglycosylation enzymes did not lead to further reduction of the apparent molecular weight of the corona proteins on the SDS-PAGE (Figure S6).

To identify the proteins that underwent deglycosylation, the deglycosylated and control coronas after enzymatic reaction *in situ* for 120 min were separated by SDS-PAGE. On the basis of the change of electrophoretic mobility, 6 regions from the lanes of control and deglycosylated coronas were excised from the SDS-PAGE. The proteins were extracted by in-gel tryptic digestion and identified using electrospray liquid chromatography mass spectrometry (LC-MS/MS) equipped with a HPLC and a Q-Exactive. The criteria for

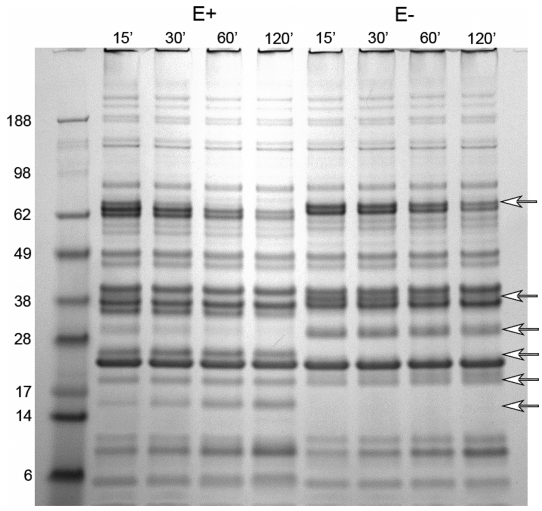

Figure 2. SDS-PAGE of protein coronas recovered from SiO_2 nanoparticles following incubation with human plasma and subsequent enzymatic deglycosylation *in situ* for various time periods (15, 30, 60, and 120 min, respectively, E+). E− represents the equivalent nonenzyme-treated controls. Arrows indicate the bands that have shifted between E− and E+. Molecular weight ladder is shown on the left (unit, kDa).

identification of deglycosylated proteins were set as follows: (1) present in both control and deglycosylated coronas; (2) shown the most significant hits (NpSpc >1); and (3) in the molecular weight ranges shown on the SDS-PAGE. A total of 20 deglycosylated proteins were identified, and the type of their glycosylation was estimated (Table 1).

Next, we sought to examine the structure of glycans in the protein corona. Because of their remarkable diversity and complexity, it is challenging and laborious to fully reveal the detailed glycan structures. The structure elucidation of even simple glycans requires highly sophisticated technical expertise and instrumentation. Thus, here we employed glycan-binding lectins to probe specific glycan structures in the protein corona. Generally, two major forms of glycosylation are present in human plasma proteins, N-linked and O-linked glycosylation (Scheme 2).[32] N-glycans are covalently linked to asparagine residues of proteins, whereas O-glycans are conjugated to serine or threonine.[28] Generally, N-glycosylation starts from a mannose-rich core structure, and subsequently undergoes a series of adding, trimming and branching monosaccharides, such as galactose (Gal) and *N*-acetylneuraminic acid (Neu5Ac), to create N-glycan structures. Similarly, O-glycosylation involves sequential addition of monosaccharides catalyzed by various glycosyltransferases. In this study, three different fluorescently labeled lectins (wheat germ agglutinin (WGA), peanut agglutinin (PNA), and concanavalin A (Con A)) were chosen to probe the glycans structures. Although these lectins have a broad specificity, WGA selectively recognizes Neu5Ac and chitobiose (GlcNAc1β-4GlcNAc), PNA binds to Gal, and Con A associates with

TABLE 1. List of the Most Abundant Deglycosylated Proteins Identified by Mass Spectrometry after Enzymatic Deglycosylation Reaction *In Situ*

accession	M_w (Da)	protein	glycosylation description
P02671|FIBA	94 973	Fibrinogen alpha chain	N- and O-linked
P00747|PLMN	90 569	Plasminogen	N- and O-linked
P02787|TRFE	77 064	Serotransferrin	N-linked
P01042|KNG1	71 957	Kininogen-1	N- and O-linked
Q9NQ79|CRAC1	71 421	Cartilage acidic protein 1	O-linked
P00748|FA12	67 792	Coagulation factor XII	N- and O-linked
P0419|HRG	59 578	Histidine-rich glycoprotein	N-linked
P05155|IC1	55 154	Plasma protease C1 inhibitor	N- and O-linked
P04004|VTNC	54 306	Vitronectin	N-linked
P08670|VIME	53 652	Vimentin	O-linked
P01871|IGHM	51 790	Ig mu chain C region	N-linked
P0073|HPT	45 205	Haptoglobin	N-linked
P01876|IGHA1	37 655	Ig alpha-1 chain C region	N- and O-linked
Q03591|FHR1	37 651	Complement factor H-related protein 1	N-linked
P02649|APOE	36 154	Apolipoprotein E	N- and O-linked
P01857|IGHG1	36 106	Ig gamma-1 chain C region	N-linked
Q15485|CN2	34 001	Ficolin-2	N-linked
O7563|FCN3	32 903	Ficolin-3	N-linked
P02647|APOA1	30 778	Apolipoprotein A-I	N-linked
P05090|APOD	21 276	Apolipoprotein D	N-linked

mannose (Scheme 2). The deglycosylated and control nanoparticle−protein complexes were incubated with the lectins individually and subsequently the lecting binding was measured as the mean fluorescence intensity by flow cytometry. The nanoparticle−protein complexes post incubation with lectins were analyzed by DCS to ensure that the lectins did not induce nanoparticle aggregation under these conditions (Figure S7). In comparison with nanoparticles coated with bovine serum albumin, which serves as a nonglycosylated control,[33] the full plasma corona showed binding only to WGA (Figure 3). This suggests that Neu5Ac is exposed on the corona surface, whereas Gal or mannose is not presented. Upon deglycosylation, the nanoparticle−protein complexes showed a significant decrease of WGA fluorescence intensity (Figure 3a), suggesting rapid removal of the surface Neu5Ac monosaccharides even after 15 min of enzymatic reaction. Conversely, the deglycosylation of the corona following 120 min incubation led to increased binding to PNA, while by contrast deglycosylation at shorter time intervals (15, 30, and 60 min) did not significantly increase the PNA binding (Figure 3b). The increased binding to PNA after an extended deglycosylation time suggests that Gal monosaccharides are gradually exposed on the corona surface with the loss of outermost glycans. It is also noted that the deglycosylated coronas did not exhibit any significant difference in Con A binding affinity compared with the nonenzymatic controls (Figure 3c), suggesting that mannose is not accessible following the deglycosylation procedure used in this study. Taken together, the

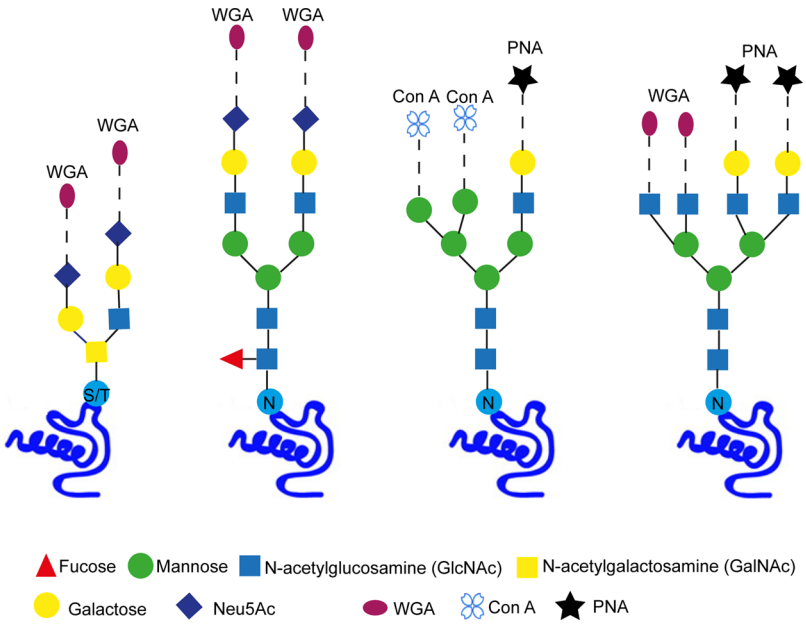

Scheme 2. O-linked and N-linked glycan structures on human plasma proteins, and the glycan-binding specificity of three types of lectins. S/T: serine or threonine; N: asparagine.

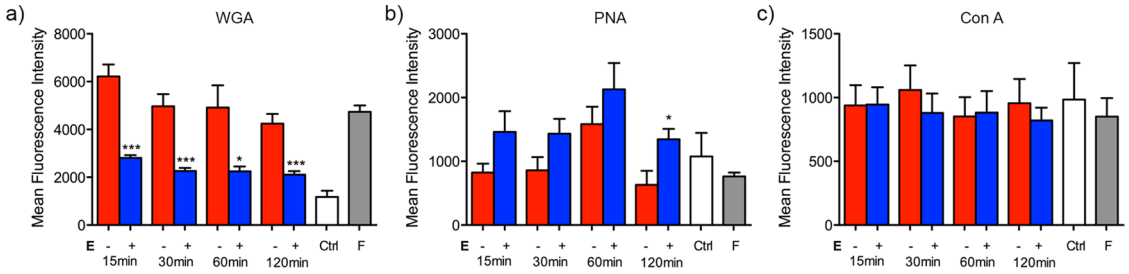

Figure 3. Lectin binding profiles of SiO_2 nanoparticle−protein complexes obtained following deglycosylation for different time periods: WGA (a), PNA (b), and Con A (c). Nanoparticles coated with BSA were used as negative controls (labeled as ctrl), and full protein corona-nanoparticles were referred to as F. Nanoparticle−protein complexes were incubated with fluorescently labeled lectins at 25 °C for 30 min. The mean fluorescence intensity of nanoparticles was measured by flow cytometry. Data are the mean ± standard error of six independent experiments. *$p < 0.05$, ***$p < 0.001$ (paired t test between E− and E+).

lectin binding profile, coupled with the SDS-PAGE data (Figure 2), indicates that the surface glycans on the protein corona undergo progressive removal upon enzymatic deglycosylation *in situ*, which leads to exposure of internal glycans that are not available on the surface of the full corona.

Glycosylation plays an important role in regulating immunity. Alterations of attached glycans can both positively and negatively modulate a number of immune pathways.[34] In the context of serum proteins, a well-known example is that of immunoglobulin G (IgG) glycovariants that exhibit different binding affinities for Fcγ receptors (FcγRs) to modulate pro- and anti-inflammatory IgG functionality. For example, sialylation-rich IgG, which has a decreased affinity for the classical FcγRs, promotes an anti-inflammatory response,[35] whereas IgG bearing a bisecting *N*-acetylglucosamine (GlcNAc) with an increased affinity for FcγRIII accelerates the development of collagen-induced arthritis.[36] To evaluate the roles of the surface glycans in nanoparticle-immune cell interactions, we differentiated and polarized monocytic THP-1 cells into pro-inflammatory M1 and anti-inflammatory M2 macrophages using an established protocol described previously to represent two major and opposing macrophage functionalities.[36] Briefly, the M1 phenotype is induced by pro-inflammatory milieu (*e.g.*, interferon-γ). In contrast, polarization to M2 macrophages often involves interleukin-4.[37] In general M1 macrophages mount potent microbicidal immune responses, whereas M2 macrophages play important roles in homeostasis and tissue repairing.[37] The deglycosylated nanoparticle−protein complexes were dispersed in serum free medium and incubated with M1- or M2-macrophages at 4 °C for 1 h to allow binding to the cell membrane without internalization. In the case of M1-macrophages, the nanoparticle−protein complexes with shorter deglycosylation reaction times (15, 30, and 60 min) did not show significant difference in cell membrane adhesion compared with

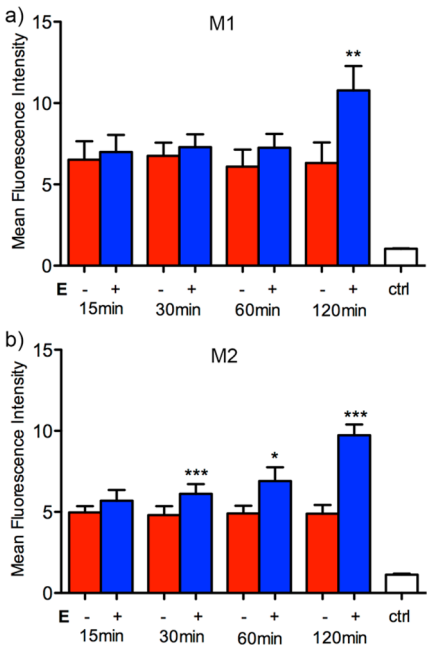

Figure 4. Cell membrane adhesion of fluorescent SiO_2 nanoparticle−protein complexes to M1 (a) and M2 (b) macrophages in serum free media. Nanoparticle−protein complexes were treated with glycosidases for various time periods (15, 30, 60, and 120 min, respectively). E− represents the equivalent nonenzyme-treated controls. Subsequently, cells were incubated with the resulting nanoparticles (100 μg mL^{-1}) at 4 °C for 1 h, followed by washing with PBS to remove excess unbound nanoparticles. The mean fluorescence intensity of cells was measured by flow cytometry, and untreated cells were used as controls (labeled as ctrl). Data are the mean ± standard error of three independent experiments, each performed in duplicate. *p < 0.05, **p < 0.01, ***p < 0.001 (paired t test between E− and E+).

the nonenzyme controls (Figure 4a). However, the further loss of glycans (deglycosylation for 120 min) resulted in an increase of cell membrane adhesion (Figure 4a). Consistently, the deglycosylation of the protein corona led to an enhanced cell membrane adhesion to the M2-macrophages (Figure 4b). Several possible underlying mechanisms can play a role in the increased adhesion of the deglycosylated nanoparticle−protein complexes on the cell membrane. The removal of glycans on the surface of the protein corona potentially has pleiotropic effects. First, the loss of glycans can reduce the steric repulsion between the corona-nanoparticles and the macrophage cell membrane, increasing nonspecific interactions. Second, it can expose underlying glycans or new epitopes, which in turn induces specific interactions with receptors that recognize modified endogenous molecules (*e.g.*, scavenger receptors) in macrophages. It is also noted that M2-macrophages appeared to be more sensitive to the loss of the glycans compared with M1-macrophages, as the partial removal of glycans after the deglycosylation reaction for 30 min already significantly increased the adhesion to M2-macrophage membrane. The distinct cell membrane properties between M1- and M2-macrophages can be one of the possibilities for their difference in the sensitivity to glycans. It is well-known that M1-macrophages express high levels of FcγRI, whereas M2-macrophages express abundant amounts of mannose receptor and scavenger receptor CD163.[37] Such molecular traits are likely to define the extent of the enhanced nonspecific and/or specific interactions occurring between the nanoparticle−protein complexes and the cell membrane.

In general, elevated cell membrane adhesion is expected to facilitate cell membrane wrapping, leading to an increase in cell uptake of nanoparticles.[6] To evaluate the effect of glycans in the protein corona on cell uptake, the nanoparticle−protein complexes were incubated with M1- or M2-macrophages at 37 °C in serum free media for various time intervals. For these studies, the nanoparticle−protein complexes that were deglycosylated for 120 min were chosen, as they resulted in enhanced cell membrane adhesion in both M1- and M2-macrophages. The full glycosylated and deglycosylated protein coronas post incubation with serum free media were analyzed by SDS-PAGE to ensure that desorption of the proteins was minimal under the conditions (Figure S8). The extent of uptake was measured by the mean fluorescence intensity of cells as a function of time over 5 h in serum free medium. The flow cytometry data showed essentially linear uptake kinetics for all the different nanoparticle−protein complexes (Figure 5). Importantly, the deglycosylated nanoparticle−protein complexes exhibited a higher uptake both in M1- and M2-macrophages at all time intervals (Figure 5), which is consistent with the observation of enhanced cell membrane adhesion. It is also noted that under the same treatment conditions, M2-macrophages showed a higher mean fluorescence intensity than M1-macrophages, suggesting that more nanoparticles were internalized by M2-macrophages (Figure 5). Studies have shown that the effect of macrophage polarization on phagocytosis is dependent on targets. In comparison to M1 macrophages, M2 macrophages show greater phagocytosis of myelin,[38] apoptotic cells,[39] latex beads,[39] and dextran.[40] A future study on the direct comparison of gene expression profiles between M1 and M2 macrophages, in particular key molecules involved in phagocytosis, is likely to shed light on the higher endocytic capability of the nanoparticle−protein complexes in M2 macrophages.

Next, we sought to investigate potential pro- or anti-inflammatory effects of macrophages in relation to nanoparticle internalization. The serum free media were collected after incubation of the nanoparticle−protein complexes with M1- or M2-macrophages at 37 °C for 5 h. Production of pro-inflammatory cytokines—human interleukin-1β (hIL-1β) and human tumor necrosis factor-α (hTNF-α), as well as an anti-inflammatory cytokine human transforming growth factor-β1 (hTGF-β1)—was measured in culture medium by an

enzyme-linked immunosorbent assay (ELISA). As expected, M1 macrophages were found to express significantly higher levels of hIL-1β and hTNF-α in comparison to M2 macrophages (Figure 6). In M1 macrophages, the uptake of nanoparticle−protein complexes (including both glycosylated and deglycosylated corona-nanoparticles) led to an increase of hIL-1β and hTNF-α, but a reduction of hTGF-β1 (Figure 6a−c). Compared with the fully glycosylated nanoparticle−protein complexes (referred to as M1+E− in Figure 6), deglycosylation of the protein corona resulted in a further increase of hIL-1β and a decrease of hTGF-β1 in M1 macrophages (Figure 6a,c), suggesting that deglycosylated nanoparticle−protein complexes promote a pro-inflammatory milieu. Consistently, the pro-inflammatory cytokine hTNF-α was elevated in M2 macrophages after exposure to deglycosylated corona-nanoparticles (Figure 6e) compared with the full corona-nanoparticles. The pro-inflammatory properties of nanoparticles have been reported previously due to various underlying mechanisms, including oxidative stress,[41] activation of Mac-1 pathway,[23] and recognition by scavenger receptors.[25] Detailed analysis of the molecular mechanisms for the up-regulation of pro-inflammatory cytokines and down-regulation of anti-inflammatory cytokine after exposure to deglycosylated nanoparticle−protein complexes remain a subject of future investigations.

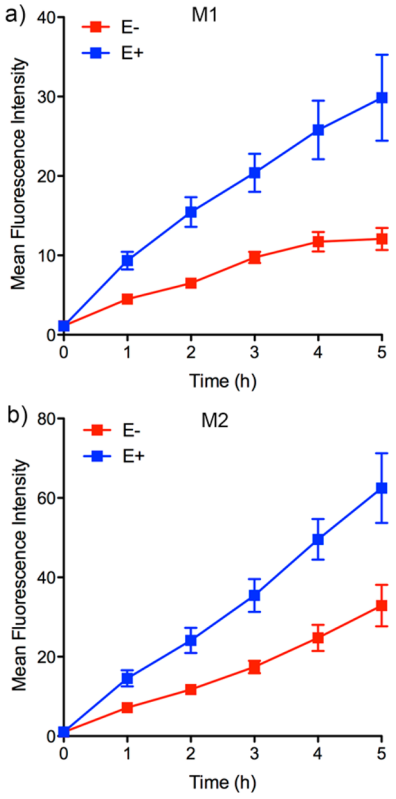

Figure 5. Cell uptake of fluorescent SiO_2 nanoparticle−protein complexes by M1 (a) and M2 (b) macrophages in serum free media. Nanoparticle−protein complexes were treated with glycosidases for 120 min (E+), and the nonenzyme-treated control is shown as E−. Subsequently, cells were incubated with the resulting nanoparticles (25 μg mL^{-1}) at 37 °C, 5% CO_2 for various time intervals, followed by washing with PBS to remove excess unbound nanoparticles. The mean fluorescence intensity of cells was measured by flow cytometry. Data are the mean ± standard error of three independent experiments, each performed in duplicate.

CONCLUSIONS

Glycosylation is one of the most frequent post-translational modifications of proteins, and confers a diversity of structural and functional properties. The present study provides the first investigation on the impact of glycosylation of a protein corona on the physicochemical properties of nanoparticles and their cellular interactions. First, a series of deglycosylated protein coronas on SiO_2 nanoparticles were obtained

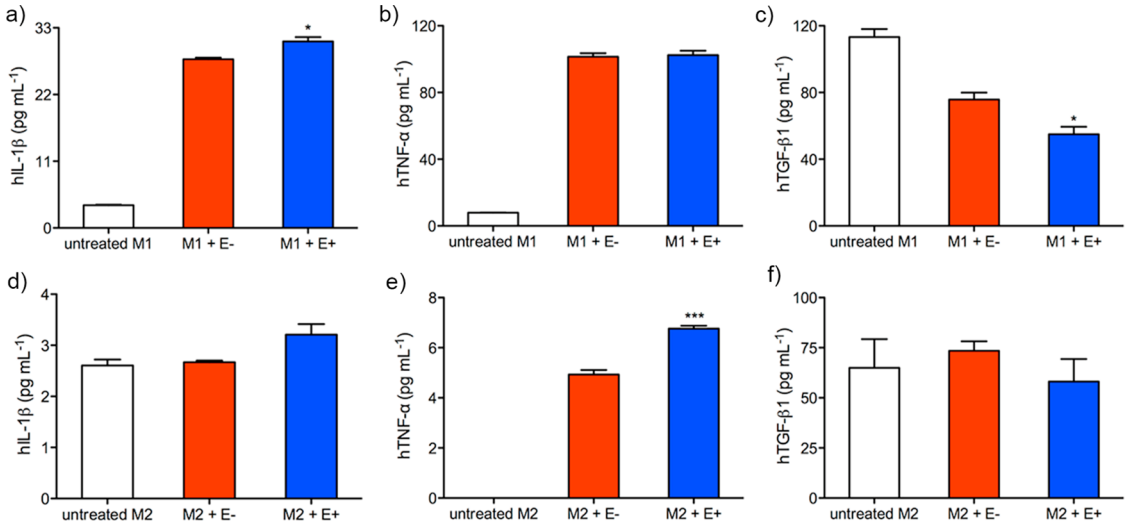

Figure 6. Cytokine expression by M1 (a−c) and M2 (d−f) macrophages. Nanoparticle−protein complexes were treated with glycosidases for 120 min (E+), and the nonenzyme-treated control is shown as E−. Subsequently, cells were incubated with the resulting nanoparticles (25 μg mL^{-1}) at 37 °C, 5% CO_2 for 5 h. The supernatant was harvested, and cytokines were measured in duplicate. Data are expressed as mean ± standard error. *$p < 0.05$, ***$p < 0.001$ (unpaired t test between E− and E+).

by enzymatic deglycosylation *in situ* of the hard corona-nanoparticles. A progressive loss of the outermost surface glycans of the protein corona was characterized by SDS-PAGE and profiled by lectin binding. Our data show that the *in situ* deglycosylation leads to partial removal of the glycans in the protein corona, which decreases the colloidal stability of nanoparticle−protein complexes. The resulting deglycosylated nanoparticle−protein complexes have been shown to enhance cell membrane adhesion to two types of THP-1 differentiated macrophages (polarized to M1 and M2), leading to an increase in nanoparticle uptake. Further, the deglycosylated corona-nanoparticles exhibit pro-inflammatory properties compared with the fully glycosylated form, suggesting the importance of glycosylation in the immunological interactions of nanoparticles. It is also worth noting that the formation of protein coronas is strongly influenced by nanoparticle size and surface chemistry.[29] Hence, the degree of glycosylation of protein coronas and the effect of cellular interactions may vary depending on physicochemical properties of nanoparticles. To fully elucidate the roles of glycans in a protein corona with respect to nanoparticle−cell recognition, receptor activation, and signal transduction, future studies will be aimed at characterizing the glycan repertoire of a given corona. Moreover, since proteins undergo a variety of post-translational modifications (*e.g.*, phosphorylation, acetylation, and methylation), this study exemplifies how such covalent addition to proteins can have biological significance for the nanoparticle protein corona, increasing their diversity and complexity.

METHODS

Materials. Tetraethyl orthosilicate (TEOS), 3-Aminopropyl trimethoxysilane, Fluorescein Isothiocyanate (Isomer I) (FITC), L-Arginine and IGEPAL CO-520 were all purchased from Sigma-Aldrich and used as received. Commercially sourced SiO_2 nanoparticles were purchased from Kisker (Steinfurt, Germany). Roswell Park Memorial Institute 1640 containing GlutaMax (RPMI), heat-inactivated fetal bovine serum (HI-FBS), Phosphate-Buffered Saline (PBS), NuPAGE Bis-Tris Precast Gel 4−12%, NuPAGE MES SDS Running Buffer, NuPAGE LDS Sample Buffer, NuPAGE Sample Reducing Agent, SeeBlue Plus2 Prestained Protein Standard, SimpleBlue SafeStain, IL-1β, TNF-α, and TGF-β human ELISA kits, AF633-wheat germ agglutinin (AF633-WGA), AF633-concanavalin A (AF633-Con A), and AF647-peanut agglutinin (AF647-PNA) were purchased from Life Technologies. Interleukin-4 (IL-4), interleukin-13 (IL-13), lipopolysaccharide (LPS), and interferon-γ (IFN-γ) were purchased from Invivogen. Phorbol 12-myristate 13-acetate (PMA) were purchased from Sigma-Aldrich. Human plasma was purchased from BioreclamationIVT. Ultrapure water with resistance greater than 18 MΩ cm was obtained from an inline Millipore RiOs/Origin system (Millipore Corporation, USA).

FITC Conjugate. *N*-1-(3-Trimethoxysilylpropyl)-*N*′-fluoresceyl thiourea (FITC-APTMS) conjugate solution was prepared by dissolving 2 mg of FITC in 2 mL of anhydrous ethanol. 10 μL of APTMS (11 × molar excess) was then added immediately to this solution and the mixture then shaken at room temperature in the dark for 4 h. This reaction was monitored by 1 H NMR (CD_3OD) where a shift in the signal from the proton adjacent to the amine group ($Si(OCH_3)_3CH_2CH_2CH_2NH_2$) upon coupling FITC reached an integration value constant and equal to the aromatic FITC signal. The reaction was deemed complete at 4 h.

SiO_2 Nanoparticle Syntheses. Fluorescent SiO_2 nanoparticles (56 nm) were prepared as follows. SiO_2 nanoparticles (5.9 g) were added to aqueous ammonia (28% w/w) and supplied with methanol to a total volume of 50 mL while rapidly stirred. 1 mL of the FITC conjugate solution was then added to this mixture followed 1 min later by 1.9 mL of TEOS. The reaction was sealed and stirred at 40 °C for a further 3 h. The particles were washed three times by centrifugation at 14000*g* for 20 min with resuspension in ethanol and water using bath sonication (Branson 1510) for each washing cycle. The resulting pellet was resuspended in water to give a final volume of 25 mL. Mass concentration was measured following vacuum drying at 600 °C for 12 h.

Preparation of Hard Protein Corona of SiO_2 Nanoparticles. Nanoparticles (30 μL, concentration 17 mg mL^{-1}) were incubated with human plasma (470 μL) at 37 °C for 1 h with continuous agitation. After incubation, the nanoparticles−protein complex was pelleted from excess plasma by centrifugation at 18000*g*, 4 °C for 20 min. The supernatant was discarded and the pellet was then resuspend in 500 μL PBS and centrifuged again to pellet nanoparticles−protein complex. The washing procedure removes unbound and loosely bound proteins from nanoparticles. The hard corona-nanoparticles are obtained after repeating the washing step three times.

Deglycosylation of SiO_2 Nanoparticle Protein Corona. Deglycosylation of the protein coronas was performed *in situ* using Protein Deglycosylation Mix (New England Biolabs) as per the manufacturer's instructions. Briefly, approximate 500 μg of SiO_2 nanoparticle−protein complexes in were suspended in 50 μL of reaction buffer containing 1 μL of deglycosylation enzyme mix. The reaction mixture was incubated at 37 °C for various time periods. After the reaction, the samples were immediately replaced on ice to slow down the reaction, and centrifuged at 18000*g*, 4 °C for 20 min. The supernatant was discarded, and the nanoparticles were resuspended in PBS.

Dynamic Light Scattering. SiO_2 nanoparticle−protein complexes (250 μg mL^{-1}) were suspended in PBS at pH 7.4 and measured with Malvern PCS-4700 instrument equipped with a 256-channel correlator. The zeta potential determination was performed using a Malvern Zetasizer 3000HSa.

SDS-PAGE. The protein coronas on the nanoparticles (10 μL, concentration of 12.5 g L^{-1}) following deglycosylation were eluted by mixing with NuPAGE LDS sample buffer and NuPAGE sample reducing agent, and heating at 70 °C for 10 min as per the manufacturer's instructions. The samples were then centrifuged at 18000*g*, 4 °C for 20 min. The supernatant was then loaded into NuPAGE Bis-Tris precast gel 4−12%. The proteins were separated by gel electrophoresis in NuPAGE MES SDS Running Buffer. The gel was stained with SimplyBlue SafeStain as per the manufacturer's instructions (Life Technologies).

Identification of Deglycosylated Proteins by Mass Spectrometry. To determine the deglycosylated proteins, the gel bands with and without enzymatic treatment for deglycosylation were cut out following SDS-PAGE. The gel digestion was performed as per the described method from Shevchenko *et al.*[42] The digested peptides were then resuspended in 0.1% formic acid. Electrospray liquid chromatography mass spectrometry (LC-MS/MS) equipped with a HPLC (Surveyor, ThermoFinnigan, CA) and interfaced with a Q-Exactive (ThermoFinnigan, CA) was used to analyze peptide mixtures following trypsin digestion. Spectra were searched with Peaks 7 software (Bioinformatics Solutions Inc.) using Sequest Uniprot/Swiss-Prot database (www.expasy.org). The spectral count of each protein was then converted into a normalized spectral count (NSpC), which was calculated using the spectral counting method as the following equation:[29]

$$NSpC_k = \left(\frac{(SpC/M_w)_k}{\sum_{i=1}^{n} (SpC/M_w)_i} \right) \times 100$$

Where $NSpC_k$ is the percentage of the normalized spectral count for protein k, SpC is the spectral count, and M_w is the molecular weight (KDa) of protein k.

Lectin Binding. SiO_2 nanoparticle−protein complexes (1 mg mL^{-1} nanoparticles) were incubated with AF633-WGA, AF633-ConA, or AF647-PNA at a final concentration of 10 μg mL^{-1} at 25 °C for 30 min. After the incubation, the reaction mixture was immediately centrifuged at 18000*g*, 4 °C for 20 min to remove excess lectin from the solution. The supernatant was discarded, and the nanoparticles were resuspended in PBS. The fluorescence intensity of the nanoparticles was analyzed by flow cytometry (Accuri, BD). Results are presented as the mean fluorescence intensity of nanoparticles from triplicates measuring at least 100 000 particles for each replicate.

Cell Culture. Human monocytic leukemia cell line THP-1 (American Type Culture Collection) cells were maintained in RPMI media with the addition of 10% (v/v) HI-FBS at 37 °C in a 5% CO_2 humidified atmosphere. M1 and M2 macrophages were generated as descried previously.[36] Briefly, THP-1 cells were first differentiated into macrophages with 320 nM PMA for 6 h, and subsequently polarized with 320 nM PMA, 100 ng mL^{-1} LPS, and 20 ng mL^{-1} IFN-γ for 18 h to generate M1 macrophages. To obtain M2 macrophages, THP-1 cells were treated with 320 nM PMA for 6 h, and then cultured with 320 nM PMA, 20 ng mL^{-1} IL-4 and 20 ng mL^{-1} IL-13 for 18 h.

Cell Membrane Adhesion of Nanoparticles by Flow Cytometry. THP-1 cells were differentiated and polarized at a density of 1×10^5 cells in 0.5 mL complete growth media into 24-well plates. After differentiation and polarization, the cells were washed twice with cold PBS, and incubated with cold serum free RPMI media containing 100 μg mL^{-1} nanoparticles at 4 °C for 1 h. The treatment media were discarded, and the cells were then gently washed with PBS twice to remove unbound nanoparticles, resuspended by gentle pipetting in cold PBS, and analyzed by flow cytometry (CyFlow Space, Partec GmbH). Results are presented as the mean fluorescence intensity of cells from at least 10 000 cells for each replica.

Cellular Uptake of Nanoparticles by Flow Cytometry. THP-1 cells were differentiated and polarized at a density of 1×10^5 cells in 0.5 mL complete growth media into 24-well plates. After differentiation and polarization, the cells were washed twice with cold PBS, and incubated with prewarmed (37 °C) serum free RPMI media containing 25 μg mL^{-1} nanoparticles at 37 °C, 5% CO_2 for various time intervals. The treatment media were discarded, and the cells were then gently washed with PBS twice to remove unbound nanoparticles, resuspended by gentle pipetting in cold PBS, and analyzed by flow cytometry (CyFlow Space, Partec GmbH). Results are presented as the mean fluorescence intensity of cells from at least 10 000 cells for each replica.

Cytokine Assay. M1 and M2 macrophages were incubated with 25 μg mL^{-1} nanoparticles at 37 °C, 5% CO_2 for 5 h. The supernatant was collected and centrifuged at 18000*g* at 4 °C for 20 min to remove any remaining nanoparticles or cell debris. hIL-1β, hTNF-α, and hTGF-β1 levels in the supernatant were measured by ELISA (Life Technologies) as per the manufacturer's instructions.

Conflict of Interest: The authors declare no competing financial interest.

Acknowledgment. This work was supported by the European Union's Seventh Framework Programme (EU FP7) under grant agreement no: 309329 (NANOSOLUTIONS), the EU FP7 program HighGlycan, Grant No. 278535, SFI PI Award (12/IA/1422; awarded to K.D.), the Irish Research Council under the EMBARK scheme (RS/2011/106), the Australian Research Council under the Australian Laureate Fellowship (F.C., FL120100030), the Discovery Early Career Researcher Award (Y.Y., DE130100488), the Australian Research Council Centre of Excellence in Convergent Bio-Nano Science and Technology (CE140100036), and the University of Melbourne under the Dyason Fellowship (Y.Y.).

Supporting Information Available: Table of physiochemical characterization of SiO_2 nanoparticle−protein complexes after deglycosylation. TEM images of SiO_2 nanoparticles. DCS analysis of nanoparticle−protein complexes. SDS-PAGE of protein coronas after enzymatic deglycosylation *in situ* for extended time periods and a higher enzyme concentration. This material is available free of charge *via* the Internet at http://pubs.acs.org.

REFERENCES AND NOTES

1. Albanese, A.; Tang, P. S.; Chan, W. C. The Effect of Nanoparticle Size, Shape, and Surface Chemistry on Bbiological Systems. *Annu. Rev. Biomed. Eng.* **2012**, *14*, 1–16.
2. Mura, S.; Nicolas, J.; Couvreur, P. Stimuli-Responsive Nanocarriers for Drug Delivery. *Nat. Mater.* **2013**, *12*, 991–1003.
3. Dawidczyk, C.; Russell, L.; Searson, P. C. Nanomedicines for Cancer Therapy: State-Of-The-Art and Limitations to Preclinical Studies that Hinder Future Developments. *Front. Chem.* **2014**, 10.3389/fchem.2014.00069.
4. Pelaz, B.; Charron, G.; Pfeiffer, C.; Zhao, Y.; de la Fuente, J. M.; Liang, X. J.; Parak, W. J.; del Pino, P. Interfacing Engineered Nanoparticles with Biological Systems: Anticipating Adverse Nano−Bio Interactions. *Small* **2013**, *9*, 1573–1584.
5. Malmsten, M. Inorganic Nanomaterials as Delivery Systems for Proteins, Peptides, DNA, and SiRNA. *Curr. Opin. Colloid Interface Sci.* **2013**, *18*, 468–480.
6. Walkey, C. D.; Chan, W. C. Understanding and Controlling the Interaction of Nanomaterials with Proteins in A Physiological Environment. *Chem. Soc. Rev.* **2012**, *41*, 2780–2799.
7. Nel, A. E.; Mädler, L.; Velegol, D.; Xia, T.; Hoek, E. M. V.; Somasundaran, P.; Klaessig, F.; Castranova, V.; Thompson, M. Understanding Biophysicochemical Interactions at the Nano-Bio Interface. *Nat. Mater.* **2009**, *8*, 543–557.
8. Cedervall, T.; Lynch, I.; Lindman, S.; Berggård, T.; Thulin, E.; Nilsson, H.; Dawson, K. A.; Linse, S. Understanding the Nanoparticle−Protein Corona Using Methods to Quantify Exchange Rates and Affinities of Proteins for Nanoparticles. *Proc. Natl. Acad. Sci. U. S. A.* **2007**, *104*, 2050–2055.
9. Tenzer, S.; Docter, D.; Kuharev, J.; Musyanovych, A.; Fetz, V.; Hecht, R.; Schlenk, F.; Fischer, D.; Kiouptsi, K.; Reinhardt, C.; *et al.* Rapid Formation of Pasma Protein Corona Critically Affects Nanoparticle Pathophysiology. *Nat. Nanotechnol.* **2013**, *8*, 772–781.
10. Casals, E.; Pfaller, T.; Duschl, A.; Oostingh, G. J.; Puntes, V. F. Hardening of the Nanoparticle−Protein Corona in Metal (Au, Ag) and Oxide (Fe_3O_4, CoO, and CeO_2) Nanoparticles. *Small* **2011**, *7*, 3479–3486.
11. Dobrovolskaia, M. A.; Patri, A. K.; Zheng, J.; Clogston, J. D.; Ayub, N.; Aggarwal, P.; Neun, B. W.; Hall, J. B.; McNeil, S. E. Interaction of Colloidal Gold Nanoparticles with Human Blood: Effects on Particle Size and Analysis of Plasma Protein Binding Profiles. *Nanomed. Nanotechnol. Biol. Med.* **2009**, *5*, 106–117.
12. Liu, W.; Rose, J.; Plantevin, S.; Auffan, M.; Bottero, J.-Y.; Vidaud, C. Protein Corona Formation for Nanomaterials and Proteins of A Similar Size: Hard or Soft Corona? *Nanoscale* **2013**, *5*, 1658–1668.
13. Scopelliti, P. E.; Borgonovo, A.; Indrieri, M.; Giorgetti, L.; Bongiorno, G.; Carbone, R.; Podesta, A.; Milani, P. The Effect of Surface Nanometre-Scale Morphology on Protein Adsorption. *PLoS One* **2010**, *5*, e11862.
14. Chanana, M.; Rivera Gil, P.; Correa-Duarte, M. A.; Liz-Marzán, L. M.; Parak, W. J. Physicochemical Properties of Protein-Coated Gold Nanoparticles in Biological Fluids and Cells before and after Proteolytic Digestion. *Angew. Chem., Int. Ed.* **2013**, *52*, 4179–4183.
15. Monopoli, M. P.; Åberg, C.; Salvati, A.; Dawson, K. A. Biomolecular Coronas Provide the Biological Identity of Nanosized Materials. *Nat. Nanotechnol.* **2012**, *7*, 779–786.
16. Treuel, L.; Brandholt, S.; Maffre, P.; Wiegele, S.; Shang, L.; Nienhaus, G. U. Impact of Protein Modification on the Protein Corona on Nanoparticles and Nanoparticle−Cell Interactions. *ACS Nano* **2014**, *8*, 503–513.
17. Hu, W.; Peng, C.; Lv, M.; Li, X.; Zhang, Y.; Chen, N.; Fan, C.; Huang, Q. Protein Corona-Mediated Mitigation of Cytotoxicity of Graphene Oxide. *ACS Nano* **2011**, *5*, 3693–3700.

18. Han, X.; Corson, N.; Wade-Mercer, P.; Gelein, R.; Jiang, J.; Sahu, M.; Biswas, P.; Finkelstein, J. N.; Elder, A.; Oberdörster, G. Assessing the Relevance of *in Vitro* Studies in Nanotoxicology by Examining Correlations Between *in Vitro* and *in Vivo* Data. *Toxicology* **2012**, *297*, 1–9.
19. Maiorano, G.; Sabella, S.; Sorce, B.; Brunetti, V.; Malvindi, M. A.; Cingolani, R.; Pompa, P. P. Effects of Cell Culture Media on the Dynamic Formation of Protein−Nanoparticle Complexes and Influence on the Cellular Response. *ACS Nano* **2010**, *4*, 7481–7491.
20. Aggarwal, P.; Hall, J. B.; McLeland, C. B.; Dobrovolskaia, M. A.; McNeil, S. E. Nanoparticle Interaction with Plasma Proteins as it Relates to Particle Biodistribution, Biocompatibility and Therapeutic Efficacy. *Adv. Drug Delivery Rev.* **2009**, *61*, 428–437.
21. Lesniak, A.; Fenaroli, F.; Monopoli, M. P.; Aberg, C.; Dawson, K. A.; Salvati, A. Effects of the Presence or Absence of a Protein Corona on Silica Nanoparticle Uptake and Impact on Cells. *ACS Nano* **2012**, *6*, 5845–5857.
22. Salvati, A.; Pitek, A. S.; Monopoli, M. P.; Prapainop, K.; Bombelli, F. B.; Hristov, D. R.; Kelly, P. M.; Åberg, C.; Mahon, E.; Dawson, K. A. Transferrin-Functionalized Nanoparticles Lose Their Targeting Capabilities When A Biomolecule Corona Adsorbs on the Surface. *Nat. Nanotechnol.* **2013**, *8*, 137–143.
23. Deng, Z. J.; Liang, M.; Monteiro, M.; Toth, I.; Minchin, R. F. Nanoparticle-Induced Unfolding of Fibrinogen Promotes Mac-1 Receptor Activation and Inflammation. *Nat. Nanotechnol* **2011**, *6*, 39–44.
24. Fleischer, C. C.; Payne, C. K. Nanoparticle−Cell Interactions: Molecular Structure of the Protein Corona and Cellular Outcomes. *Acc. Chem. Res.* **2014**, *47*, 2651–2659.
25. Yan, Y.; Gause, K. T.; Kamphuis, M. M.; Ang, C. S.; O'Brien-Simpson, N. M.; Lenzo, J. C.; Reynolds, E. C.; Nice, E. C.; Caruso, F. Differential Roles of the Protein Corona in the Cellular Uptake of Nanoporous Polymer Particles by Monocyte and Macrophage Cell Lines. *ACS Nano* **2013**, *7*, 10960–10970.
26. Bohne-Lang, A.; Von der Lieth, C. W. GlyProt: *in Silico* Glycosylation of Proteins. *Nucleic Acids Res.* **2005**, *33*, W214–W219.
27. Moremen, K. W.; Tiemeyer, M.; Nairn, A. V. Vertebrate Protein Glycosylation: Diversity, Synthesis and Function. *Nat. Rev. Mol. Cell Biol.* **2012**, *13*, 448–462.
28. Paszek, M. J.; DuFort, C. C.; Rossier, O.; Bainer, R.; Mouw, J. K.; Godula, K.; Hudak, J. E.; Lakins, J. N.; Wijekoon, A. C.; Cassereau, L.; *et al.* The Cancer Glycocalyx Mechanically Primes Integrin-Mediated Growth and Survival. *Nature* **2014**, *511*, 319–325.
29. Monopoli, M. P.; Walczyk, D.; Campbell, A.; Elia, G.; Lynch, I.; Baldelli Bombelli, F.; Dawson, K. A. Physical-Chemical Aspects of Protein Corona: Relevance to *in Vitro* and *in Vivo* Biological Impacts of Nanoparticles. *J. Am. Chem. Soc.* **2011**, *133*, 2525–2534.
30. Hühn, D.; Kantner, K.; Geidel, C.; Brandholt, S.; De Cock, I.; Soenen, S. J.; Rivera_Gil, P.; Montenegro, J.-M.; Braeckmans, K.; Müllen, K.; *et al.* Polymer-Coated Nanoparticles Interacting with Proteins and Cells: Focusing on the Sign of the Net Charge. *ACS Nano* **2013**, *7*, 3253–3263.
31. Walczyk, D.; Bombelli, F. B.; Monopoli, M. P.; Lynch, I.; Dawson, K. A. What the Cell "Sees" in Bionanoscience. *J. Am. Chem. Soc.* **2010**, *132*, 5761–5768.
32. Preston, R. J.; Rawley, O.; Gleeson, E. M.; O'Donnell, J. S. Elucidating the Role of Carbohydrate Determinants in Regulating Hemostasis: Insights and Opportunities. *Blood* **2013**, *121*, 3801–3810.
33. Swiss-Prot Database Entry P02769.
34. Johnson, J. L.; Jones, M. B.; Ryan, S. O.; Cobb, B. A. The Regulatory Power of Glycans and Their Binding Partners in Immunity. *Trends Immunol.* **2013**, *34*, 290–298.
35. Nimmerjahn, F.; Ravetch, J. V. Anti-Inflammatory Actions of Intravenous Immunoglobulin. *Annu. Rev. Immunol.* **2008**, *26*, 513–533.
36. Tjiu, J.-W.; Chen, J.-S.; Shun, C.-T.; Lin, S.-J.; Liao, Y.-H.; Chu, C.-Y.; Tsai, T.-F.; Chiu, H.-C.; Dai, Y.-S.; Inoue, H.; *et al.* Tumor-Associated Macrophage-Induced Invasion and Angiogenesis of Human Basal Cell Carcinoma Cells by Cyclooxygenase-2 Induction. *J. Invest. Dermatol.* **2008**, *129*, 1016–1025.
37. Murray, P. J.; Allen, J. E.; Biswas, S. K.; Fisher, E. A.; Gilroy, D. W.; Goerdt, S.; Gordon, S.; Hamilton, J. A.; Ivashkiv, L. B.; Lawrence, T.; *et al.* Macrophage Activation and Polarization: Nomenclature and Experimental Guidelines. *Immunity* **2014**, *41*, 14–20.
38. Durafourt, B. A.; Moore, C. S.; Zammit, D. A.; Johnson, T. A.; Zaguia, F.; Guiot, M. C.; Bar-Or, A.; Antel, J. P. Comparison of Polarization Properties of Human Adult Microglia and Blood-Derived Macrophages. *Glia* **2012**, *60*, 717–727.
39. Chinetti-Gbaguidi, G.; Baron, M.; Bouhlel, M. A.; Vanhoutte, J.; Copin, C.; Sebti, Y.; Derudas, B.; Mayi, T.; Bories, G.; Tailleux, A.; *et al.* Human Atherosclerotic Plaque Alternative Macrophages Display Low Cholesterol Handling But High Phagocytosis Because of Distinct Activities of the PPARγ and LXRα Pathways. *Circ. Res.* **2011**, *108*, 985–995.
40. Edin, S.; Wikberg, M. L.; Rutegård, J.; Oldenborg, P.-A.; Palmqvist, R. Phenotypic Skewing of Macrophages *in Vitro* by Secreted Factors from Colorectal Cancer Cells. *PloS One* **2013**, *8*, e74982.
41. Xia, T.; Kovochich, M.; Brant, J.; Hotze, M.; Sempf, J.; Oberley, T.; Sioutas, C.; Yeh, J. I.; Wiesner, M. R.; Nel, A. E. Comparison of the Abilities of Ambient and Manufactured Nanoparticles to Induce Cellular Toxicity According to An Oxidative Stress Paradigm. *Nano Lett.* **2006**, *6*, 1794–1807.
42. Shevchenko, A.; Wilm, M.; Vorm, O.; Mann, M. Mass Spectrometric Sequencing of Proteins Silver-Stained Polyacrylamide Gels. *Anal. Chem.* **1996**, *68*, 850–858.